

We are IntechOpen, the world's leading publisher of Open Access books Built by scientists, for scientists

6,900

Open access books available

186,000

International authors and editors

200M

Downloads

Our authors are among the

154

Countries delivered to

TOP 1%

most cited scientists

12.2%

Contributors from top 500 universities



WEB OF SCIENCE™

Selection of our books indexed in the Book Citation Index
in Web of Science™ Core Collection (BKCI)

Interested in publishing with us?
Contact book.department@intechopen.com

Numbers displayed above are based on latest data collected.
For more information visit www.intechopen.com



Experimental Studies of the Electrical Nonlinear Bimodal Transmission Line

Abdou Karim Farota, Mouhamadou Mansour Faye,
Bouya Diop, Diène Ndiaye and Mary Teuw Niane

Additional information is available at the end of the chapter

<http://dx.doi.org/10.5772/intechopen.76204>

Abstract

After a few years of calm, the investigations on the dynamic, especially nonlinear, systems returned to the front of the research in non-linear physics. We propose, in this chapter, a study of an electrical nonlinear transmission line, realized in a previous work, to use the latter to highlight certain properties (modulation instability—MI, Fermi-Pasta-Ulam (FPU) recurrence, fragmentation of solitons in wave trains, multiplication (increase) and division of frequencies, etc.), which are observed in several domains in applied physics: hydraulic, artificial neuronal, network physical appearance (physics) of the plasma, and the circulation.

Keywords: nonlinear transmission line, trains of solitons, modulation instability, FPU recurrence, dispersion curve

1. Introduction

Nowadays, the study of electrical nonlinear transmission lines (NLTLs) progresses in both the theoretical field [1, 2] and technology [3–5]. The tools for the simulation of mechanical systems and the study of electrical transmission lines became a major challenge because many electronic systems have nonlinear transmission line (NLTL) modules. The experimental results presented in this chapter are part of an effort to understand the phenomena that occurs in the NLTL. We designed and built the experimental device to perform many investigations on the fundamentals that allow the understanding of the nonlinear effects. Other researchers

focused more on specialized aspects that allowed us to revisit nonlinear effects in a completely new light of research that have marked the history of nonlinear physics in particular.

In Section 2 of this chapter, we present the experimental device realized in a preceding work. In Section 3, we propose an experimental method of determination of wavelength and the velocity phase and velocity group that allowed us to trace point by point the curve dispersion of the line. The effects of fading and nonlinearity are highlighted in Section 4. The phenomenon of modulation instability (MI) is the object of Section 5. In Section 6, we discuss the follow-ups in the periodic recurrence of Fermi-Pasta-Ulam (FPU) in low and high frequencies. Section 7 is dedicated to some applications to use our experimental platform.

2. Overview of the experimental device

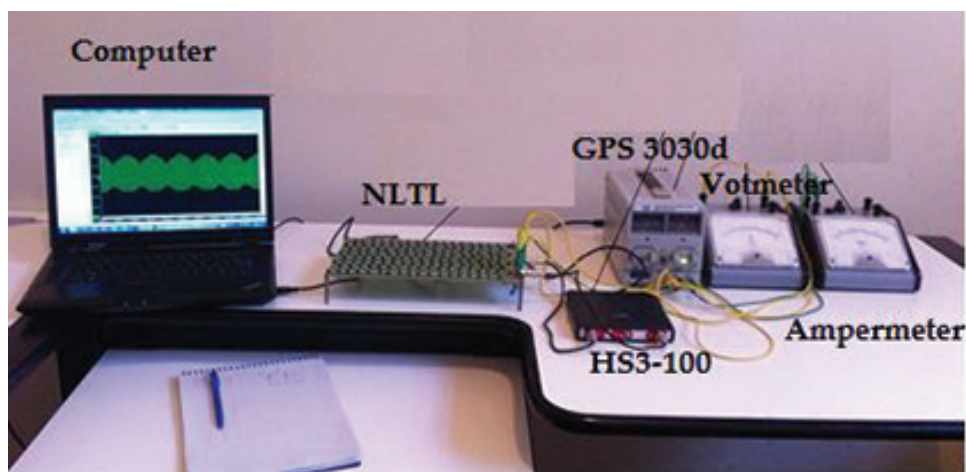


Photo 1: Experimental device.

Computer: for control, acquisition, and data processing;

NLTL: electrical nonlinear transmission line;

HS3-100: which accommodates the arbitrary signal generator and digital oscilloscope;

GPS-3030d: generator of analog tension to polarize the line;

Voltmeter: for the control of the tension of polarization of the line;

Amperemeter: for the control of the current, which crosses the line.

3. Curve dispersion

The first step in the study of an electrical transmission line is to determine its ability to convey electric waves. Indeed, the electric nonlinear transmission line like all wave guides presents a different response depending on the type of the wave introduced.

3.1. Wavelength determination

To determine the wavelength of a signal, we introduce one low amplitude sine wave in the line input in order to stay in the linear approximation (50 mV), then we put a first probe at the entrance of a cell of order n , then a second probe to a cell located at the position $n + 1$, $n + 2$ until the signals observed from the two probes are in phase. Thus, we determine the wavelength expressed in terms of cell number.

We have at the determined level the wave number k given in the relationship (Eq. (1)):

$$k = \frac{2\pi}{\lambda} \quad (1)$$

where k is expressed in rad/cel and λ is a wavelength.

However, this method is quite unclear, and it is rare to see a wavelength that is always equal to an integer multiple of the number of cells. However, this step has the advantage to confirm that the wavelength is greater than the cell, which allows considering the use of a method more precise by calculating the phase velocity of the wave.

3.2. Determination of the phase velocity

Staying in the linear approximation, we introduce the input of line at low amplitude (50 mV) sine wave and visualize the signals collected by two sensors located on two consecutive cells. We then determine the phase of the wave velocity by choosing a point of the wave, which has the same phase (e.g., maximum). This phase velocity is expressed in cell/s (Figure 1). We determine then the number of waves by the relationship (Eq. (2)):

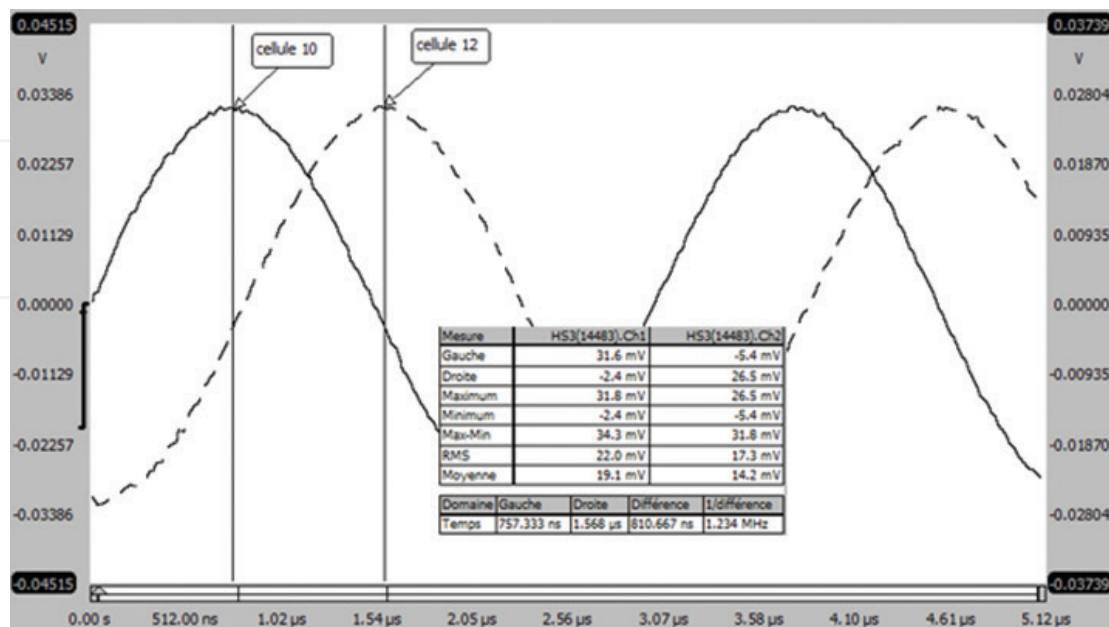


Figure 1. The phase velocity of the wave measured by taking the signals at the entrance of two inductors of the same values that are consecutive. Then we determine the difference of time between these two points, making sure that the two points of the wave are the same phase; cells 10–12, $f = 330$ kHz, $\Delta t = 810.667$ ns, $v_\varphi = 2.46$ 106 cells/s.

$$k = \frac{\omega}{v_\varphi} = \frac{2\pi f}{v_\varphi} \quad (2)$$

where f is the frequency of the incident wave and v_φ the phase velocity.

We determine then the wave number k , for all frequencies available by the system, which allow us to determine the curve dispersion of the line.

3.3. Frequency modes

We present, in **Figure 2**, the curve of dispersion obtained by the theoretical calculation [1] (solid lines) and the experimental points determined by the above-described method (filled triangles). We note a good agreement between our experimental results and the theoretical results. The frequencies of experimentally determined cuts $f_{c1} = (590 \pm 15)$ KHz, $f_{c2} = (830 \pm 20)$ KHz, and $f_{c3} = (975 \pm 25)$ KHz are in good agreement with the theoretical values $f_{c1} = 550$ KHz, $f_{c2} = 807$ KHz, and $f_{c3} = 970$ KHz, respectively. These cut-off frequencies delimit several areas of the dispersion curve, which correspond to modes of propagation of individual waves in the transmission line.

3.3.1. Low frequency mode

Low frequency (LF) mode is the branch of the curve dispersion that lies below the first cutoff frequency.

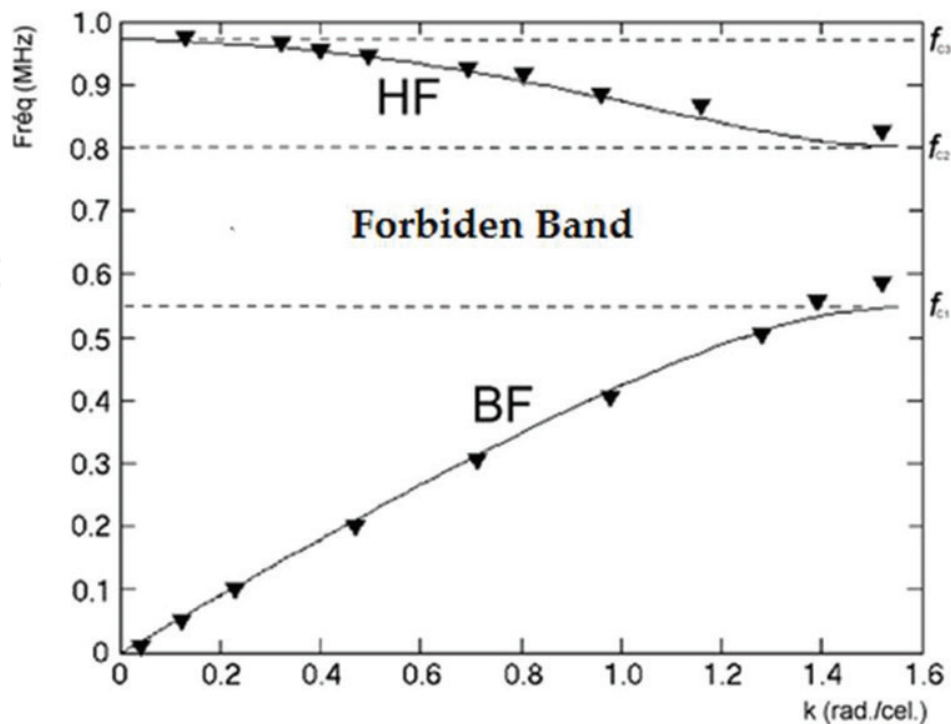


Figure 2. Comparison between the curve dispersion experimental triangles and that obtained by calculation (continuous line) for the bimodal transmission line ($L_1 = 220 \mu F$, $L_2 = 470 \mu F$ with polarization voltage of line $V_0 = 1.5$ V).

3.3.2. High frequency mode

High frequency (HF) mode is the branch of the curve of dispersion which lies between the second and the third cut-off frequency f_1 and f_2 , respectively. It is noted that practically there is no science that has managed to determine the curve dispersion in HF mode with much precision than that presented in the present work. This is due to the fact that, on the one hand, in HF mode signals are weak compared to those of the bi-frequency (BF) mode, and, on the other hand, the quality of the experimental device impacts the measures as we have used a more accurate methodology.

3.3.3. Forbidden band

The forbidden band is a range of frequency between the cut-off frequencies of f_2 and f_3 . In this area, other physical laws [1] govern the wave propagation.

4. Nonlinearity and dissipation effects on the signal

Dissipation and dispersion phenomena affect the wave propagation in nonlinear electrical line in various proportions.

4.1. Effect of dissipation

Because of the presence of dissipative element in the line, signals introduced at the entrance of the line undergo a weakening that increases with the distance traveled in the line. Impairment affects the wave in a uniform manner, it is a linear phenomenon that leads to a global change in the amplitude of the wave; however, the overall shape of the wave remains intact. In order to observe the effects of wave dissipation in the nonlinear electrical line, we have to diminish the effects of the nonlinearity. To do so, we are in an almost linear approximation by introducing into the line of very low amplitude waves.

We see, in **Figure 3**, the sine wave introduced at the entrance of the line keeps its intact shape to the 144th cell; however, we note a weakening of the signal, which sees its amplitude virtually halved.

Note, finally, that the weakening of the signal affects all signals introduced in the line. It is important to note that the HF mode signals are more sensitive to the effects of dissipation; also explained by the fact that high-frequency inductors have impedances higher than in BF mode. This often makes the phenomena more difficult to observe in the HF mode than in BF mode.

4.2. Effect of the nonlinearity

To observe the effects of nonlinearity in the nonlinear transmission electric line, the amplitude of the signal introduced into the line is increased. Indeed, by increasing the amplitude of the signal, the voltage varies significantly around the tension of polarization V_0 of the diodes varactor thus leading their operating point to move on a significant range of value around the Q_0 resting on the characteristic $C(V)$ (**Figure 4**) point. The various points of the signal, not meeting the same value of the capacity, then move at different velocity, thus leading to a dispersion of the signal.

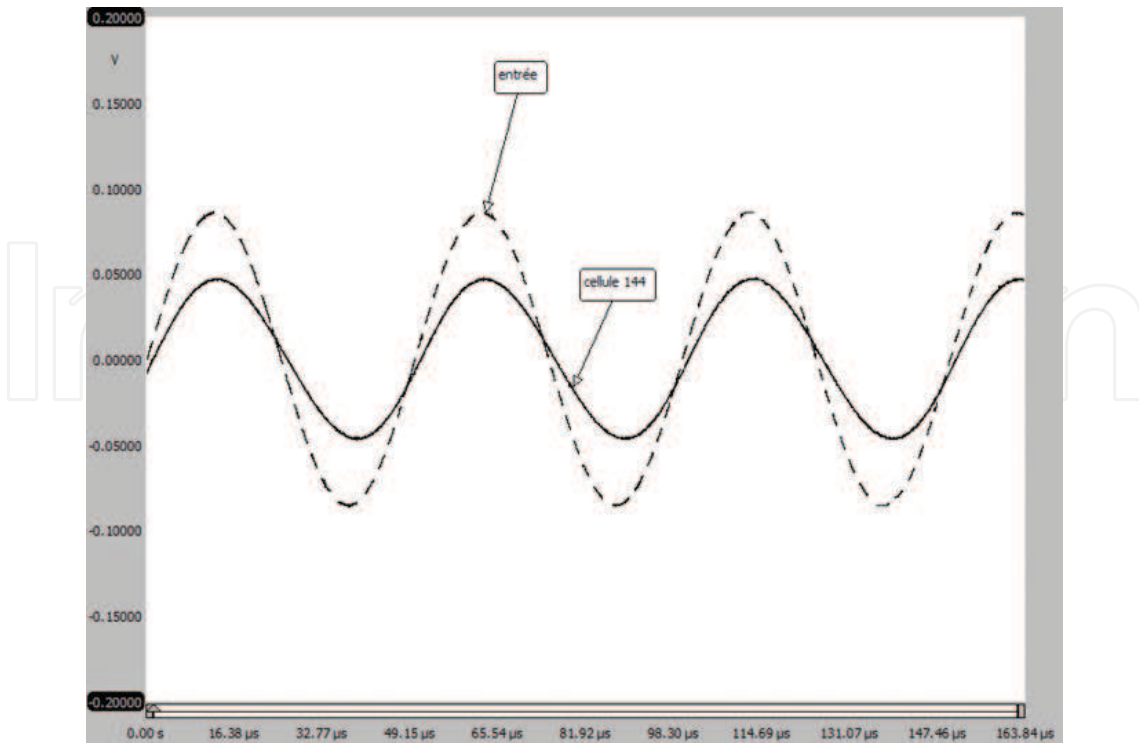


Figure 3. Evolution of an input signal of small amplitude sinusoidal shape ($f = 20$ KHz, V signal = 50 mV) after crossing a stretch of 144 cells of the nonlinear electrical line bi-inductance. Note the linear weakening of the signal keeps sinusoidal shape intact.

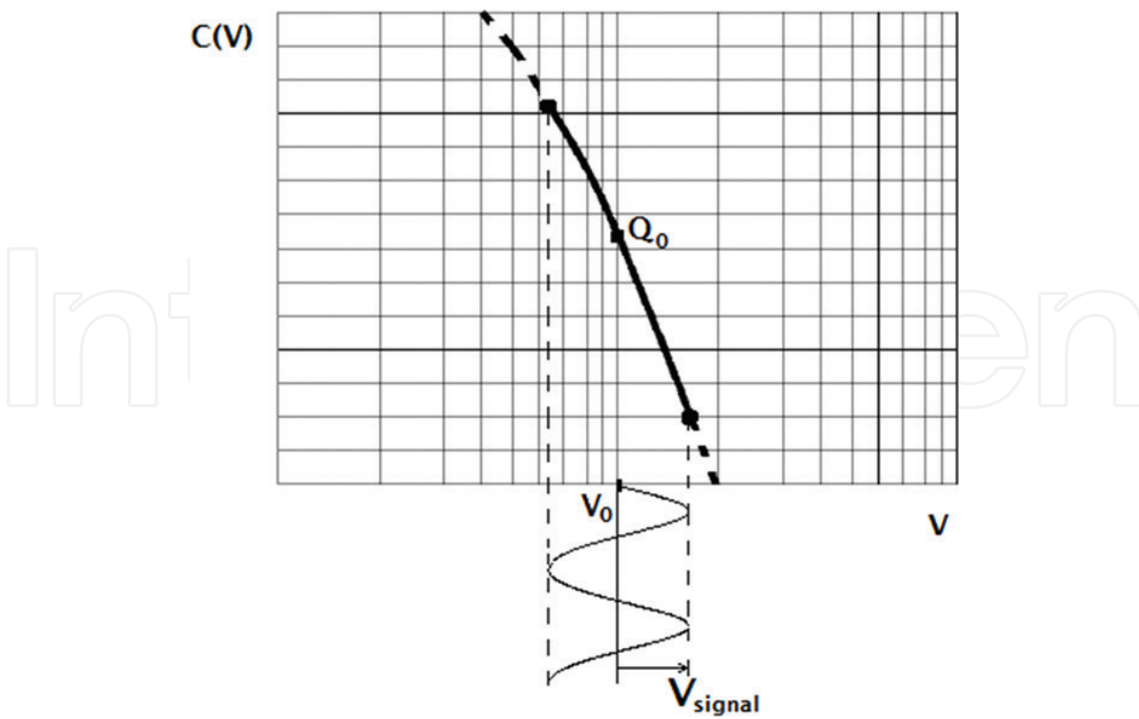


Figure 4. V_{signal} of amplitude input voltage is superimposed on the bias of the varactor diode voltage to impose on them an operating point located on the one hand and the resting point Q_0 on the other hand.

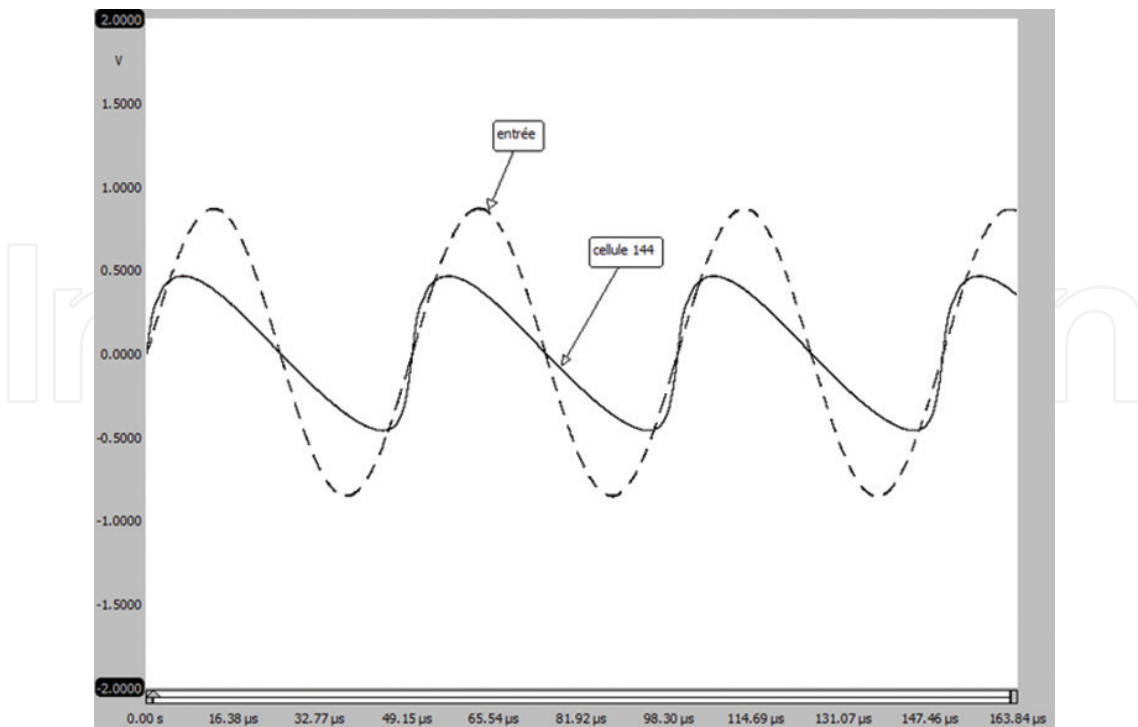


Figure 5. Nonlinearity caused by crossing a stretch of line of 144 cells induces a very strong dissymmetry of the signal, which then presents a flat forehead.

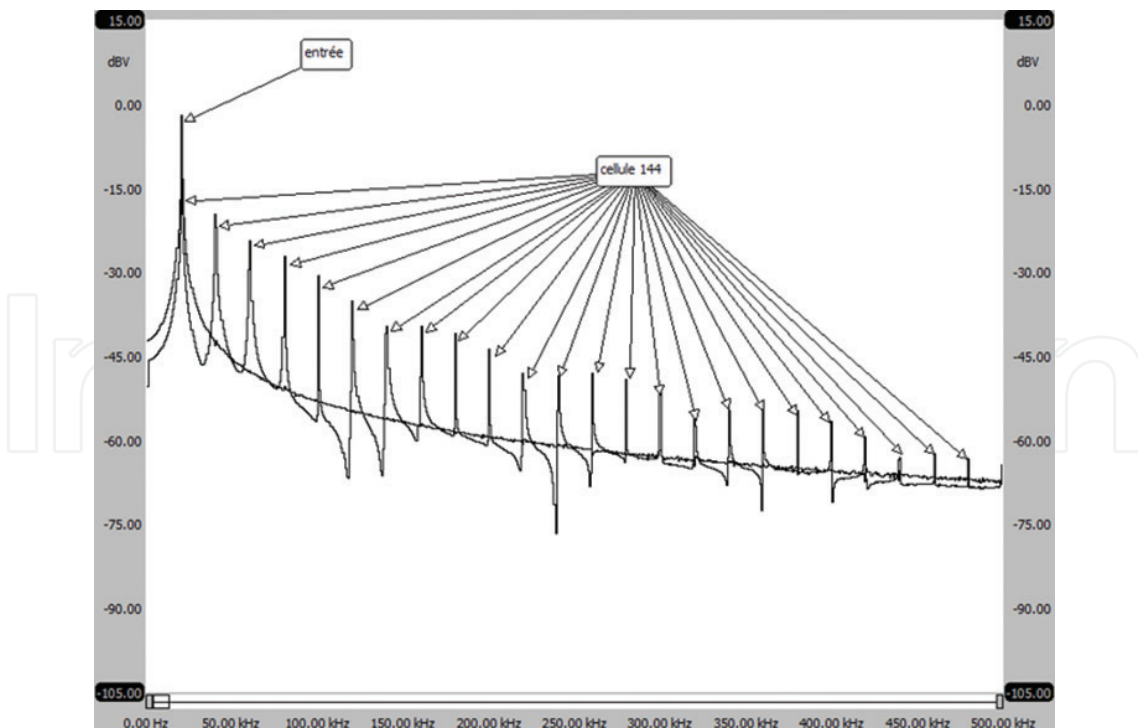


Figure 6. Illustration of the spreading of the wave in the spectral domain due to the effects of nonlinearity after crossing a section of power line nonlinear of 144 cells by a sinusoidal signal of frequency $f = 20$ kHz, amplitude $V_{\text{signal}} = 1.5$ V for a polarization of the V_0 line voltage = 1.5 V.

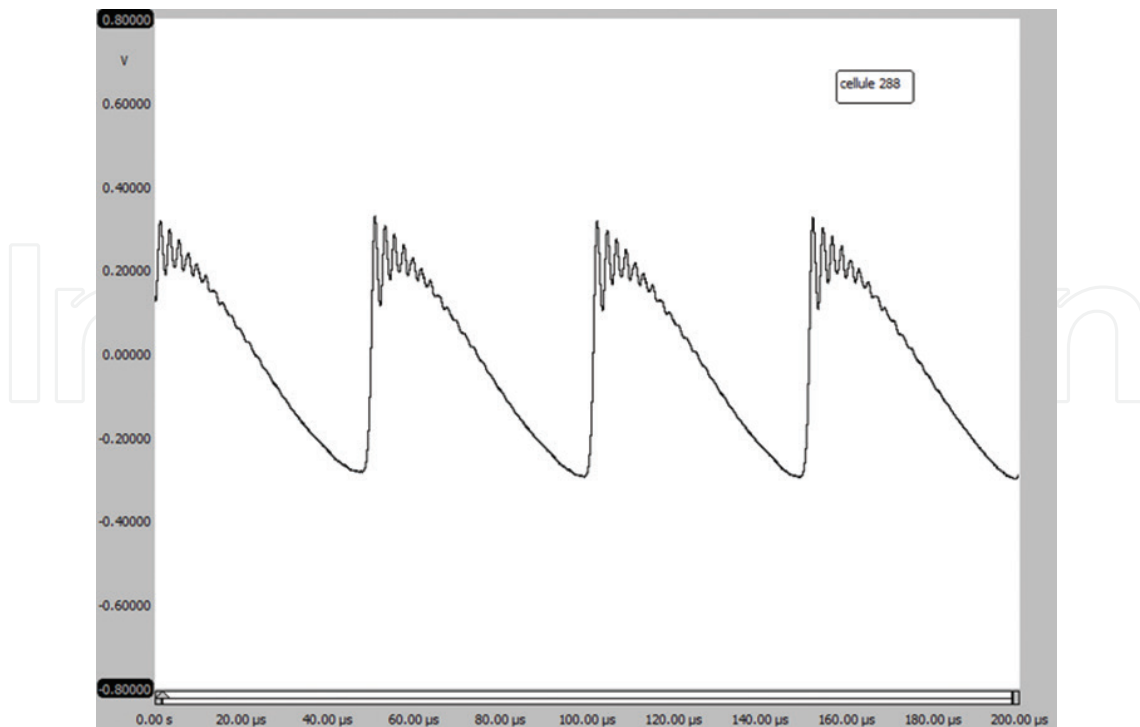


Figure 7. Destruction of the sine wave kept after crossing a section of electrical nonlinear line aft 288th cells by a sinusoidal signal of frequency $f = 20$ kHz, amplitude $V_{\text{signal}} = 1.5$ V, and a polarization of the line voltage $V_0 = 1.5$ V.

The signal can then undergo a significant distortion as it penetrates into the line. We present a characteristic effect related to the effects of nonlinearity of the signals (in **Figure 5**). It is obvious that the 144th cell wave become very asymmetrical, as phases of the various points of the wave velocity are different.

In fact, everything happens as if parts of the wave with large amplitudes are moving faster than low amplitude. The wave starts to break down; it shows more and more overtones, thus reflecting the complexity of the shape and explains why nonlinearity leads to a spreading of the wave (**Figure 6**).

Ultimately, the wave front flattens completely; called shock wave similar to the phenomenon observed in the aerodynamic field when a mobile starts to move at a speed greater than the speed of sound. At this moment, the wave breaks (**Figure 7**).

5. Modulation instability

Modulation instability (MI) is a universally known phenomenon-affecting continuum. It reflects the ability of a weakly perturbed wave to undergo very strong modulations that finally break down in a stable wave [6–8] train. Historically, the MI studied in hydrodynamic fields [9–11] and subsequently the phenomenon observed in other media of propagation of the waves such as electrical transmission lines nonlinear [12–15] optical guide. The MI can occur in space or in time domain. Benjamin and Feir were the pioneers of the study of the MI. In 1967, they studied the evolution in time of MI and demonstrated both theoretically and

experimentally that a uniform continuous wave train could be unstable to the disruptions that modulate its envelope [7, 8]. The impact of the work of Benjamin and Feir, often called instability of Benjamin-Feir, is mainly in hydrodynamics.

5.1. Criterion of modulation instability in the electrical bi-inductance line

In a previous work, Pelap [1] conducted a theoretical study of a power nonlinear transmission line bi-inductance. He first showed that the wave propagation in the line governed by an equation of type Ginzburg Landau complex (GLC) then sought solutions of the equation in discrete semi-approximation. The approach was different from that adopted by Lange and Newell for hydrodynamic fields [16] to establish a criterion of instability for a plane wave propagating through a nonlinear bi-inductance linear and weakly dissipative inductance. The wave is unstable under modulation if the pseudo-product (Eq. (3)) is positive that is:

$$P_r Q_r + P_i Q_i > 0 \tag{3}$$

where P_r , P_i , Q_r , and Q_i are, respectively, the real and imaginary coefficients of dispersion terms P and of nonlinearity Q .

If the pseudo-product (Eq. (3)) is positive, it means then that the wave is unstable under the modulation and the system will be the seat of an MI.

We study, for our electrical nonlinear bi-inductance transmission line, the evolution of the pseudo-product in HF mode (**Figure 8**) and the BF mode (**Figure 9**).

Knowledge of the values of the critical wave in the HF mode allows us to clarify if areas of the curve dispersion of the wave are stable under the modulation or not (**Figure 10**). Thus, we are building a decision tool that allows us in our different investigations to determine the frequency of the signals that we send in the line for the observation of specific phenomena properly.

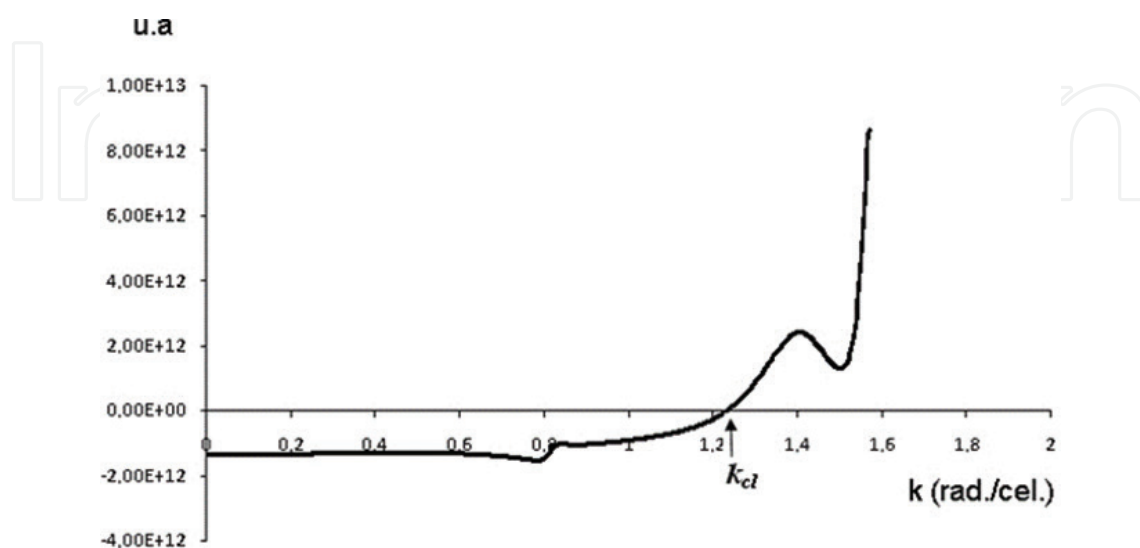


Figure 8. Shape of the pseudo-product in BF mode for the inductance bi line. The value of the wave number is critical in this mode which marks the separation between the area of stability, and the zone of instability is $k_c = 1.23305$ rad./cel.

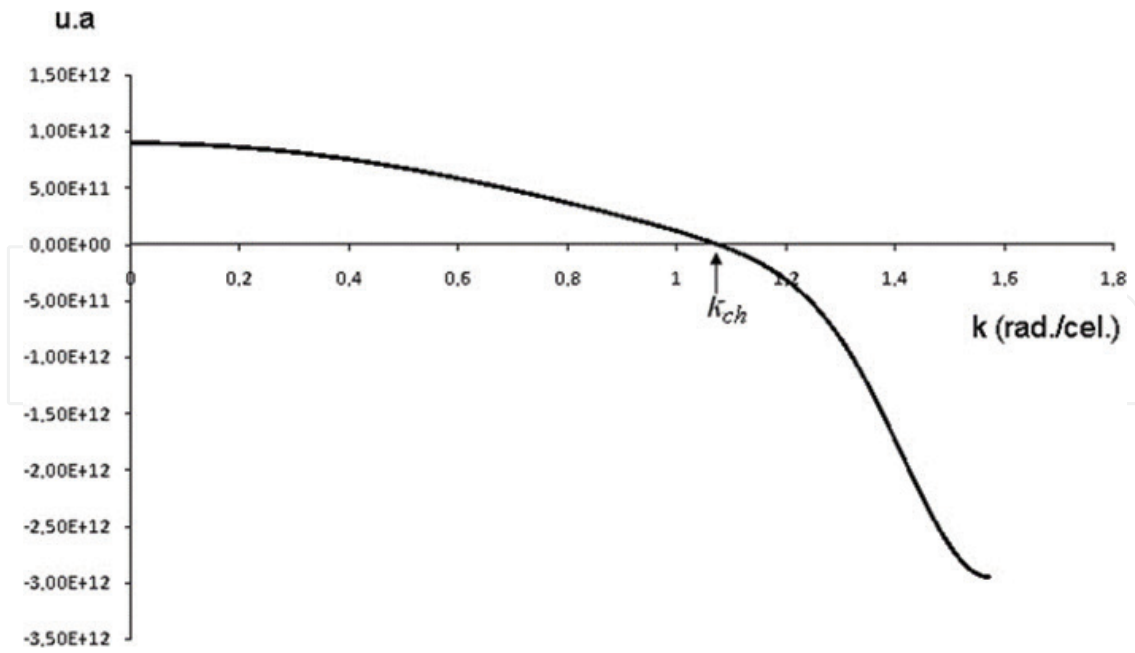


Figure 9. Changing of the pseudo-product in HF mode for the inductance bi line. The value of the wave number critical separation between the area of stability and the zone of instability in this mode is $k_{ch} = 1.07595$ rad./cel.

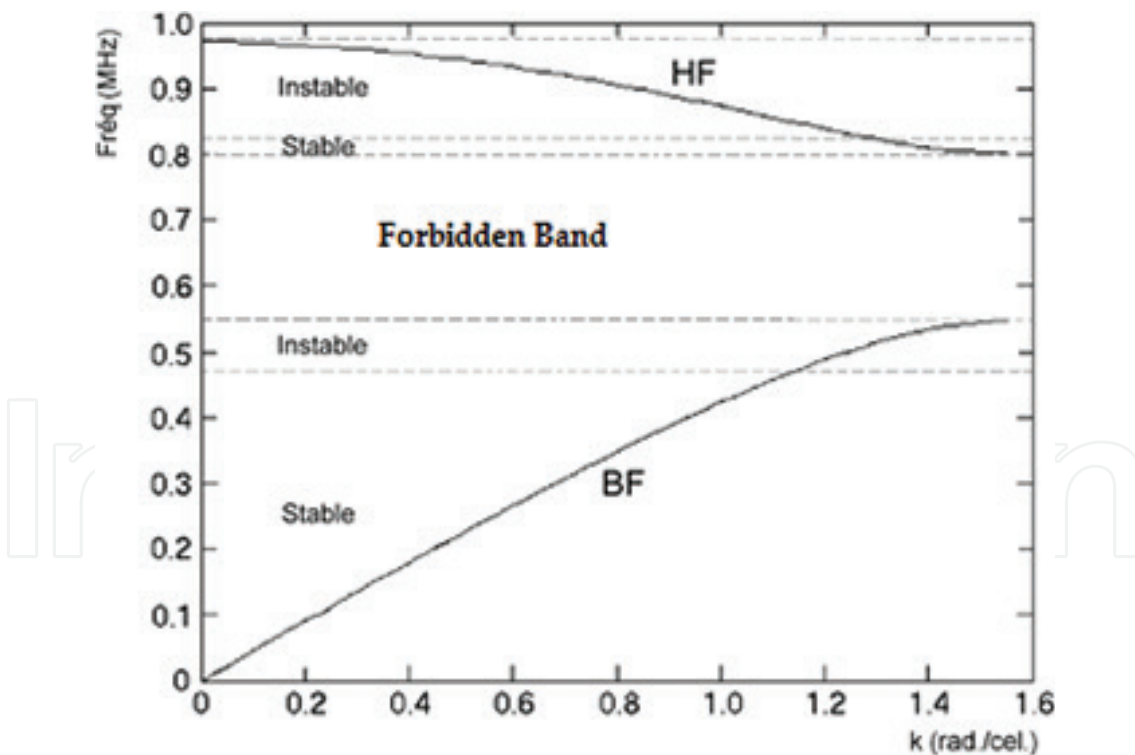


Figure 10. Delimitation of modulation areas of stability and instability of the electric nonlinear bimodal transmission line based on the criterion of modulation instability.

5.2. Observation of MI in the nonlinear bimodal transmission line

We observe modulation instability in the bi-inductance line in the BF mode. To do this, on the one hand, we must choose a signal whose frequency is in the region of modulation

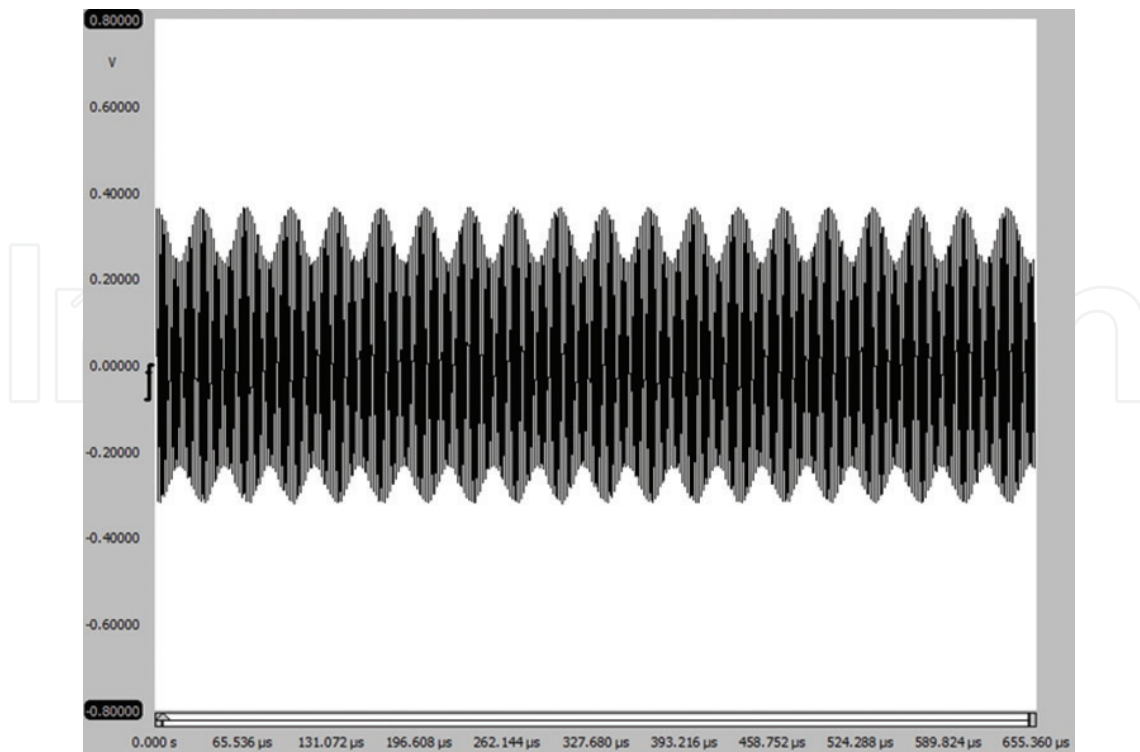


Figure 11. Observation of MI in the BF mode in the nonlinear bimodal transmission line for a signal of frequency $f = 491.5$ kHz, and amplitude $V_M = 3.6$ V observed at the 138th cell.

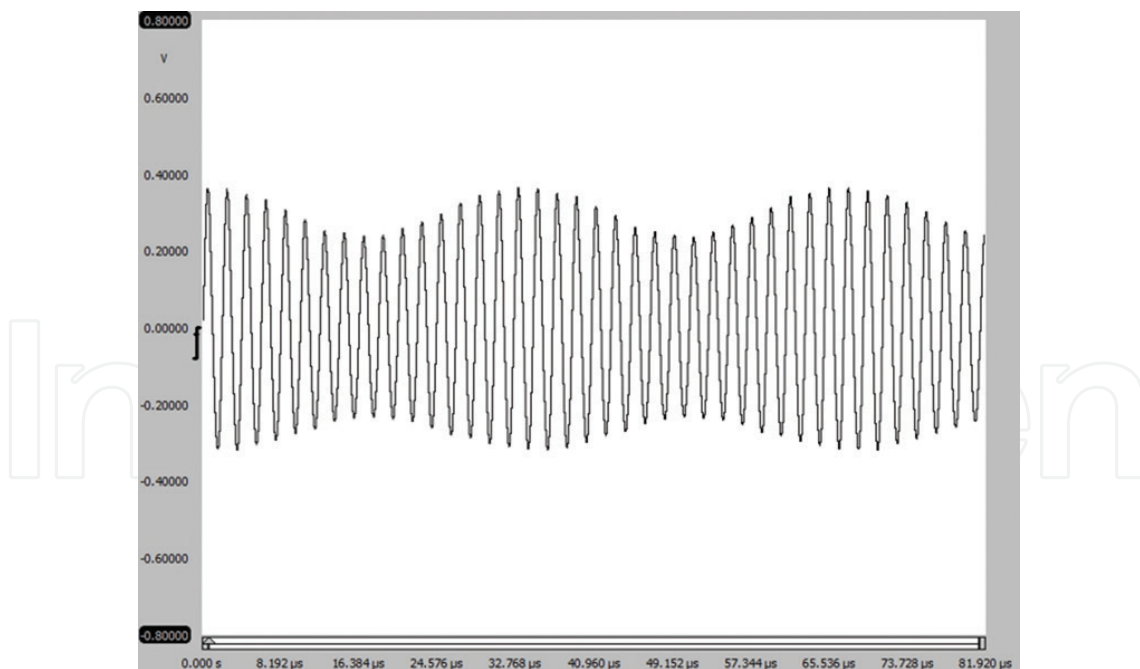


Figure 12. Details of signal in BF mode in the nonlinear bi-inductance transmission line for a signal of frequency $f = 491.5$ kHz and amplitude $V_M = 3.6$ V observed at the 138th cell. Note that wave plane of entry is modulated in amplitude ($M = 0.18$ modulation rate).

instability such as provided for in the calculations, and on the other hand, to introduce amplitude that is strong enough to initiate the disruption that will trigger the IM of the wave. To do this, we have chosen a sinusoidal signal whose frequency was $f = 491.5$ kHz for

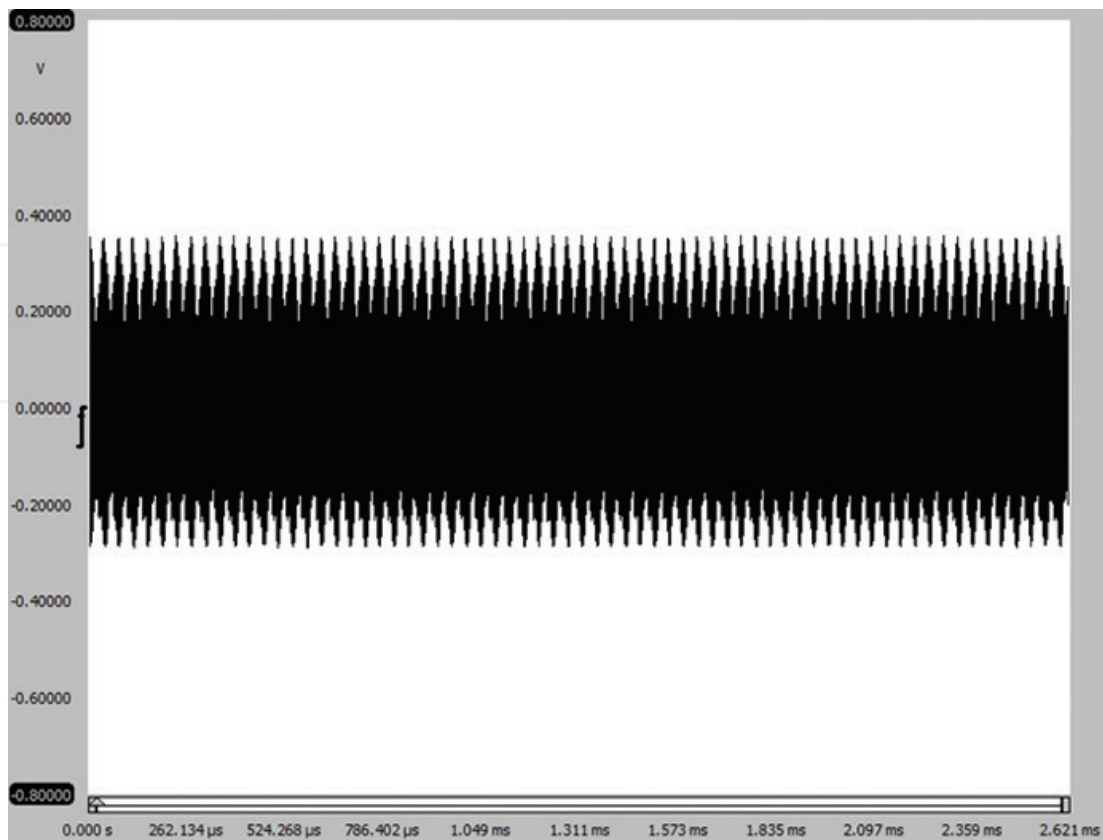


Figure 13. Observation of modulation instability in HF mode in the transmission of nonlinear bi-inductance line for a signal of frequency $f = 897$ KHz and amplitude $V_M = 3.6$ V observed at 130th cell.

amplitude $V_M = 3.6$ V. We observe in **Figure 11**, the signals are collected at the level of the 138th cell.

Zooming on the recording of the signal shows that plane wave, which is injected at the entrance to the line, shows the MI in amplitude whose rate is 0.18 (**Figure 12**).

Modulation instability was also observed in HF mode. In this case, we have chosen a signal whose frequency is in the region of modulation instability such as provided for by the calculations in HF mode and which has a magnitude large enough to initiate the disruption that will trigger the MI of the wave. To do this, we have chosen a sinusoidal signal whose frequency is $f = 897$ KHz and amplitude $V_M = 3.6$ V. We observe in **Figure 13**, the signals collected at the level of the 130th cell.

6. Fermi-Pasta-Ulam recurrence

6.1. Historical reviews

In 1952, Fermi et al. [17] led a digital experience on a nonlinear constituted 64 particle system point of identical mass related to their neighbors by springs weakly nonlinear. They expected that the introduced nonlinear coupling between neighboring oscillators would allow a transfer of energy between successive vibration modes, thus causing an equipartition of energy over a wide spectrum. Against all odds, the system introduced a quasi-periodic behavior of

the most complex. They found that all the energy which was initially excited almost returned to fundamental mode. This phenomenon was later called recurrence Fermi-Pasta-Ulam (FPU). This experience was important for two reasons—first, it highlighted the complexity of nonlinear systems; second, it demonstrated the power of the complex systems.

6.2. Experimental observation of the Fermi-Pasta-Ulam recurrence in a transmission electrical nonlinear bi-inductance line

The electrical nonlinear bimodal transmission line presents a level of complexity compared to its counterpart mono inductance as far as it has two modes of propagations, the HF and BF mode. We propose to conduct a study of the recurrence of FPU in each mode.

6.2.1. The FPU recurrence in the BF mode

In BF mode, we introduce a sine wave of frequency $f = 475$ KHz in the line with an amplitude $V_{\text{signal}} = 1.5$ V, the polarization of the line voltage is $V_0 = 1.5$ V, and we collect the signal level of the inductance of each cell L_2 (L_2 inductors are located on cells of even order). We see that the collected signal presents deformations of stochastic appearance that initially will grow as it sinks into the line to finally find the sinusoidal shape of the signal of departure to the 22nd cell (**Figure 14**). This phenomenon observed in the electrical nonlinear bimodal transmission line is known as the Fermi-Pasta-Ulam (FPU) recurrence.

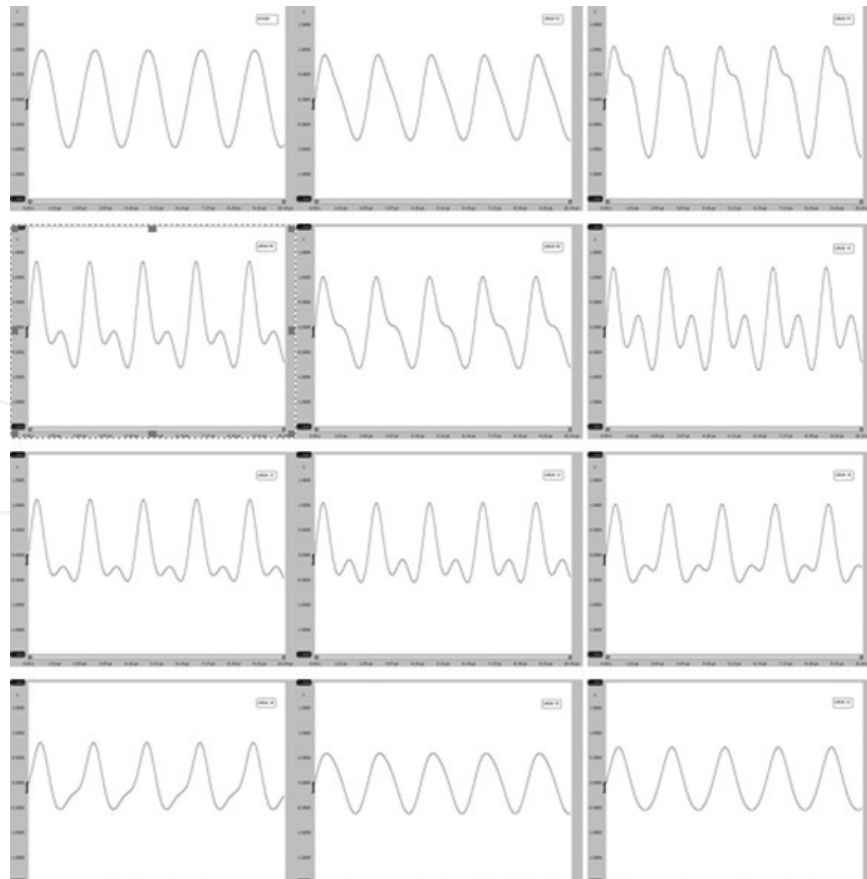


Figure 14. FPU Recurrence observed in electrical nonlinear transmission line in BF mode on inductance L_2 , for a signal of frequency $f = 475$ KHz and $V_{\text{signal}} = 1.5$ V and $V_0 = 1.5$ V as voltage polarization of the line.

We continue to find the signal in the following cells (44th, 66th, 88th, and 110th), which enabled us to confirm the return period of the line to 22nd cells (**Figure 15**).

Again, we see that the amplitude of the signals decreases by increasing order from recurrence. This is due to the joule effect because let us not forget that our line is dissipative for the presence of inductor L_1 and $r_1 = 5\Omega$ his resistor and the inductor L_2 and its $r_2 = 8\Omega$.

6.2.1.1. Comparison of the recurrence at the level of cells of inductance L_1 and L_2

We also conducted the study of signals in cells of type L_1 (chokes on the cells of odd order). We find that the period of recurrence for the inductances of L_1 type is the same as that measured for inductors of type L_2 . We present the first recurrence observed for L_2 and L_1 cells at the level of cell 22 and 23, respectively, in **Figure 16**. Later, we see that successive recurrences on the inductances of L_1 type intervene at the level of cells 45, 67, 89, 111, and so on. For inductor L_1 , we found recurrence period also at 22nd cell.

Yet the study of the evolution of the waveforms between two recurrences often shows a sensitive form between the signals taken on L_2 and those taken on L_1 . We see the signals observed at the level of cells 10 and 11 for the inductors L_1 and L_2 , respectively, are quite dissimilar in shape in **Figure 17**.

In **Figure 18**, we observe the spectral decomposition of signals collected on inductance L_2 and L_1 at cells 10 and 11, respectively. We see that the two signals contain the fundamental term

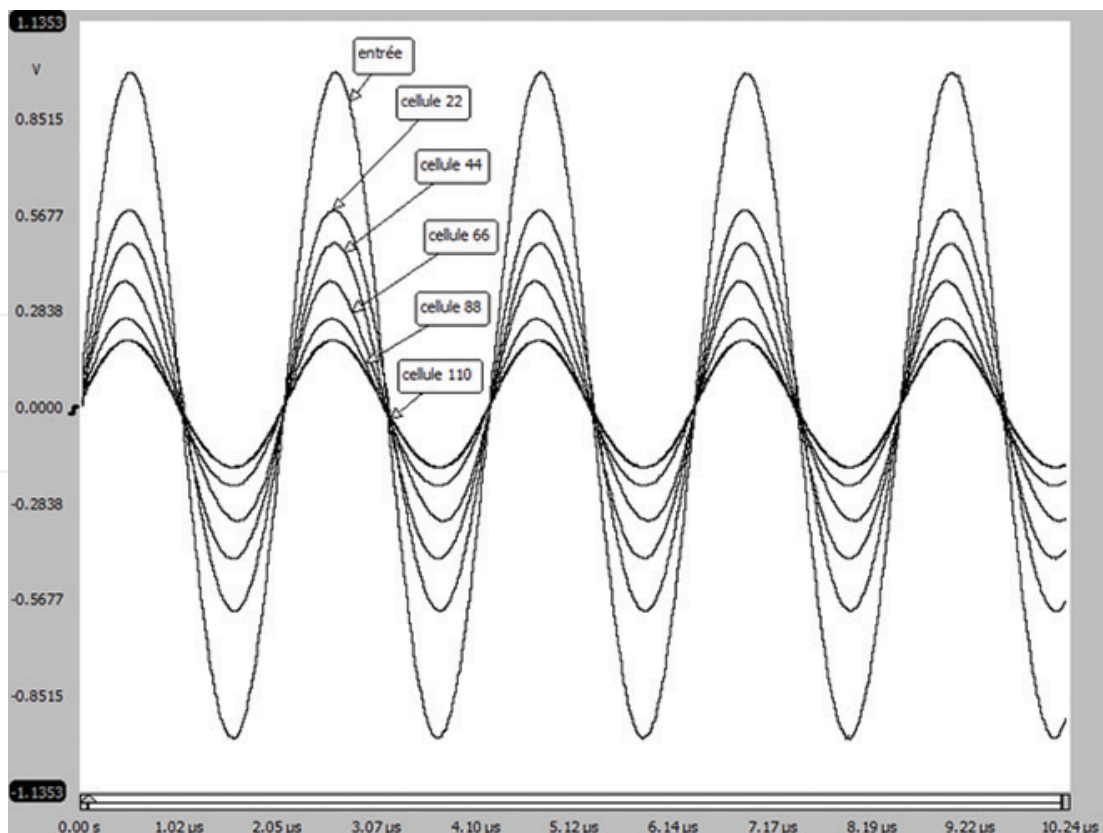


Figure 15. Observation of the first five recurrences for the electrical nonlinear bimodal transmission line in the BF for inductance L_2 , with $f = 475$ kHz, $V_{\text{signal}} = 1.5$ V, and polarization voltage of the line $V_0 = 1.5$ V.

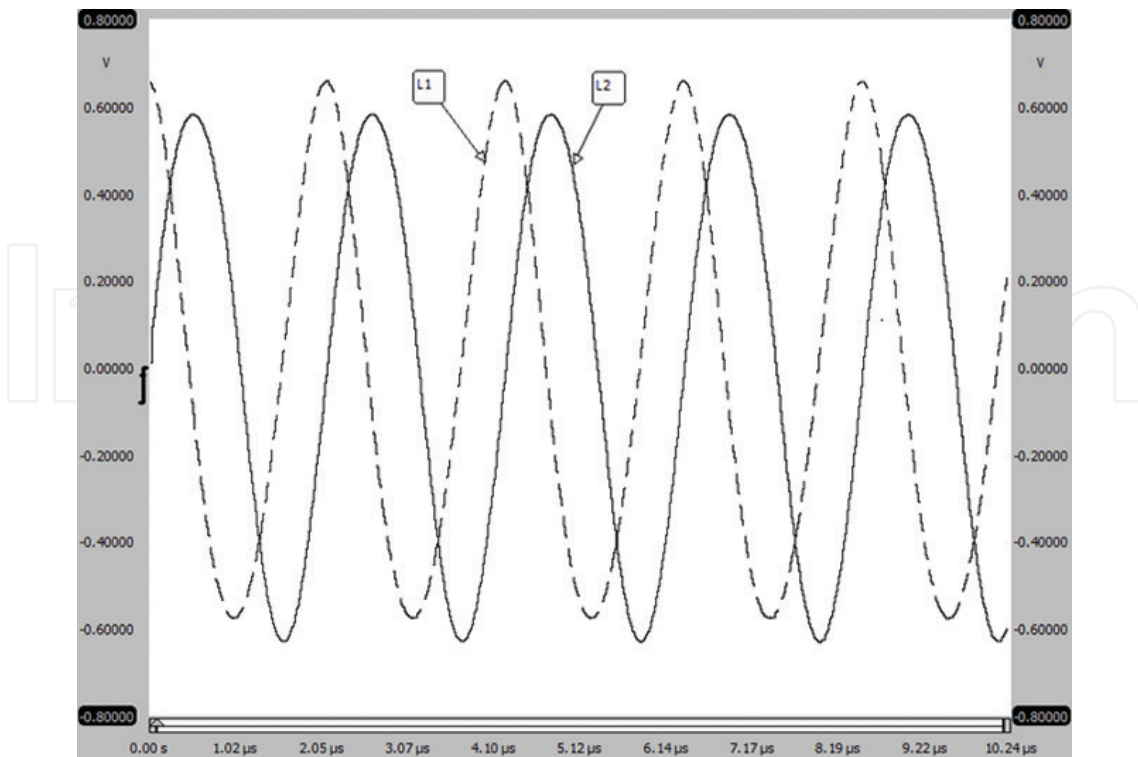


Figure 16. Observation of the first recurrence at the 22nd and 23rd cells on inductors L_1 and L_2 , respectively, for a signal in the BF mode of frequency $f = 475$ kHz and $V_{\text{signal}} = 1.5$ V, the voltage polarization of line is $V_0 = 1.5$ V.

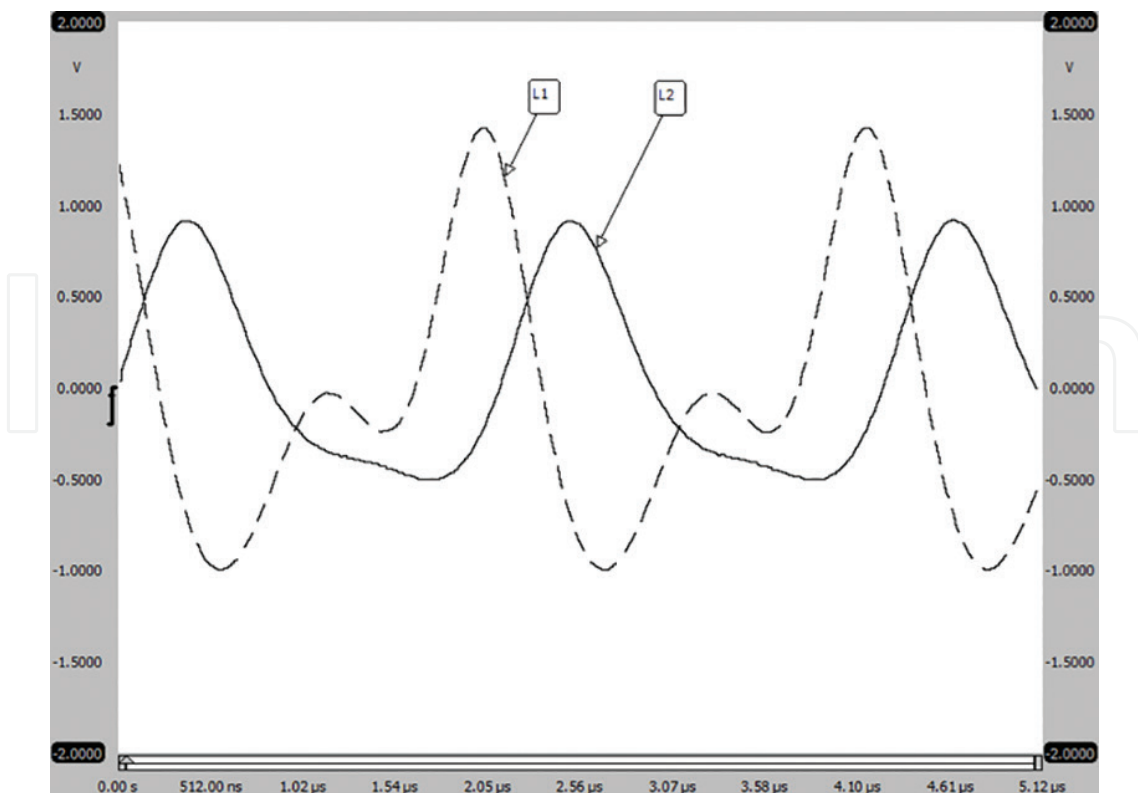


Figure 17. Observation of the signals measured on the inductance L_2 and L_1 at cells 10 and 11, respectively, for a signal in the BF mode amplitude $V_{\text{signal}} = 1.5$ V, the voltage polarization of the line $V_0 = 1.5$ V, and frequency $f = 475$ kHz.

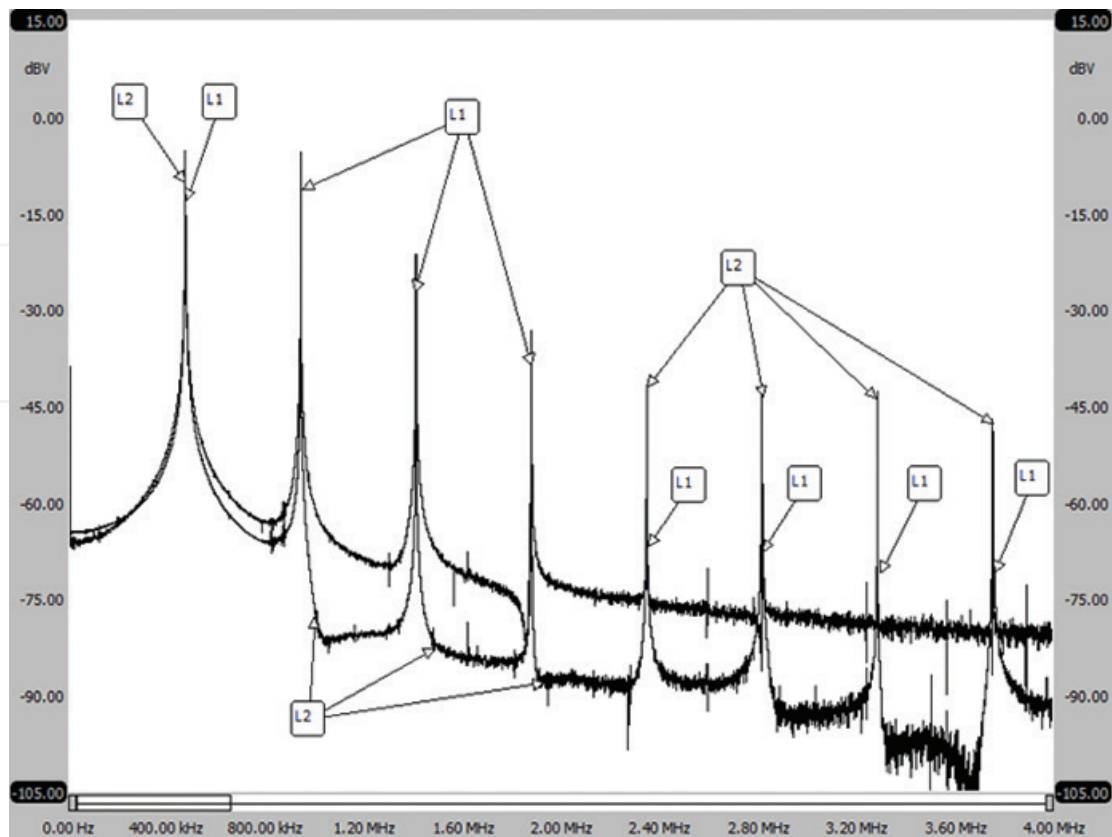


Figure 18. Observation of the Fourier transform of signals measured on the inductance L_2 and L_1 at cells 10 and 11, respectively, for a signal taken in mode BF having a frequency $f = 475$ kHz, and amplitude $V_{\text{signal}} = 1.5$ V, with a voltage polarization $V_0 = 1.5$ V.

that corresponds to the frequency of the sine wave introduced ($f = 475$ KHz) and located at frequency harmonics 940 KHz, 1.41 MHz, 1.88 MHz, and so on. We see, for that concerning the cell 10, the signal on the inductor L_2 , the contribution of the first three harmonics prevail over others in addition to the fundamental. However, with regard to the collected cell on the 11th cell, inductance L_1 , the contribution of the following harmonics are predominant in addition to the fundamental. We can deduce that signals of inductors L_1 and L_2 are in fact identical in spectral terms and that is the relative contribution of the different harmonics, which explains the difference in shape between these signals.

On the other hand, the occurrence of recurrences marks the return to the ground state of the signals observed at the level of the inductance L_1 as L_2 . In **Figure 19**, we see the fundamental term becomes predominant, the contribution of the various harmonics being then quite marginal.

6.2.2. The FPU recurrence in the HF mode

Observation of recurrent FPU in HF mode may prove to be more challenging than the BF mode. This is primarily because, in this mode, HF signal amplitude is much lower than in BF mode because of the preponderance of the dissipative effects on nonlinear effects. Let us add to it in high frequencies, the periods of recurrence are much smaller and we count the periods by units of cell. However, we observed the FPU recurrence in HF mode by substantially increasing the amplitude of the input signals. Unlike the BF mode, we have sometimes

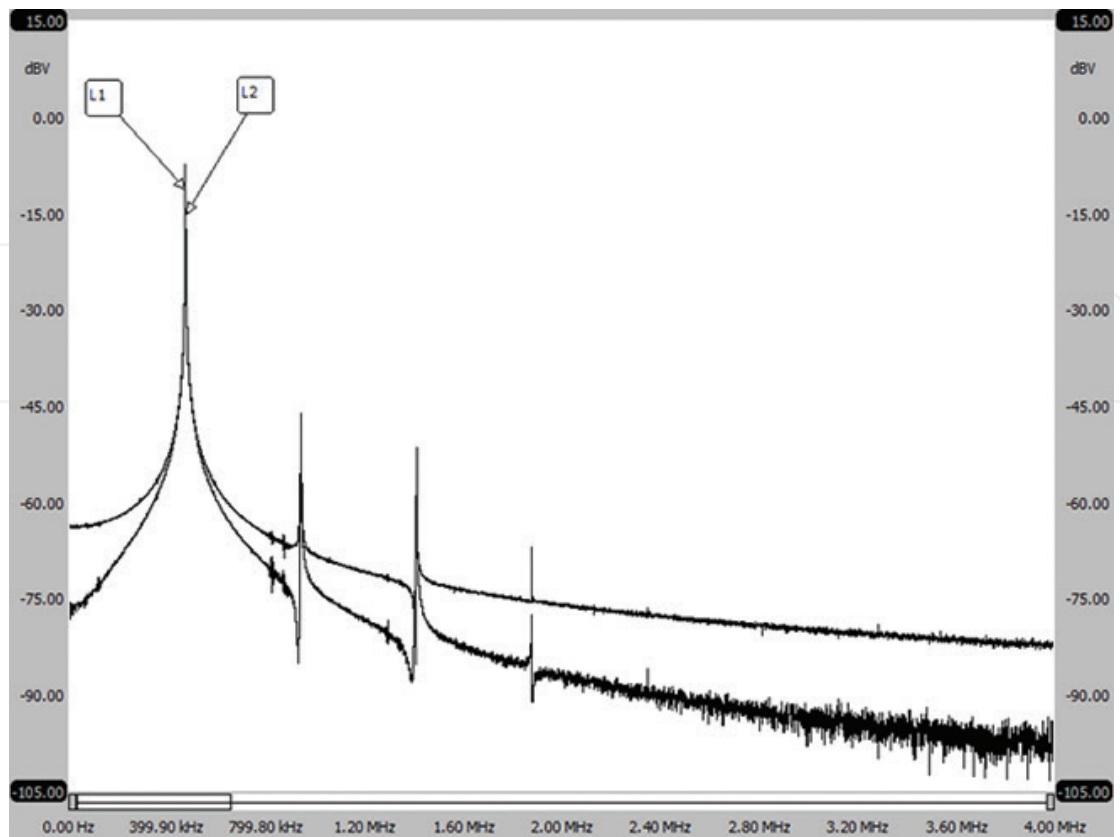


Figure 19. Observation of the Fourier transform of signals measured on inductors L_1 and L_2 in the first recurrence (cell 22 and 23, respectively) for a signal in the BF mode $f = 475$ kHz frequency and amplitude $V_{\text{signal}} = 1.5$ V for a voltage polarization $V_0 = 1.5$ V. There is a return to the ground state ($f = 475$ kHz) contribution of the harmonics of orders 1, 2, and 3 is marginal.

resorted the spectral analysis of the transform of Fourier to ensure that the wave has covered its sinusoidal shape. In precedent works [18, 19], we present the evolution of the signal and Fourier transformation (signal frequency $f = 910$ kHz, $V_{\text{signal}} = 2.2$ V and polarized voltage $V_0 = 1.5$ V). In these works, we see that the amplitude of the signal of the positive half-wave is higher than that of the wave for the negative alternation. This comes from the fact that the nonlinearity of the capacity $C(V)$ does not similarly affect the two alternations. The minimum of the negative alternation seems more flattened than the positive alternation. On the other hand, Fourier analysis reveals the presence of a harmonic with twice the fundamental frequency. We find for the inductors L_1 , located in the cells of odd order, recurrences occur to the cells 5th, 11th, 17th, 23rd, and so on. With regard to inductance L_2 , located on the cells of even order, the recurrences occur in cells 4th, 10th, 16th, 22nd, and so on. The return period of the line for the HF mode considered is therefore an average of 6th cell.

6.3. Evolution of the period of recurrence based on the amplitude of the signal

We also studied the evolution of the return period depending on the amplitude of the signal in the BF mode and frequency $f = 475$ KHz. By varying the amplitude of the input signal offered in the line, we see a linear dependence of the period of recurrence with the inverse of the square root of the amplitude of the voltage of the signal [19] (**Figure 20**). Toda [20], in the case of the electric transmission line mono-modal, determined theoretically this dependence of the return period with the amplitude of the applied signal.

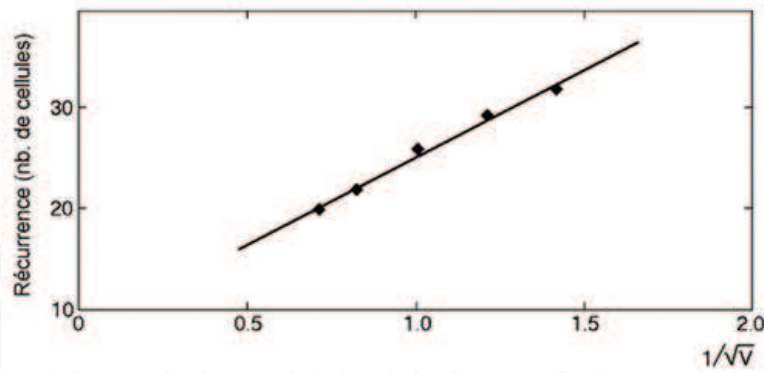


Figure 20. Variation of the return period expressed in number of cell based on the inverse of the square root of the amplitude of the signal applied to a frequency $f = 475$ KHz wave and voltage polarization $V_0 = 1.5$ V.

7. Observation of the solitons in the line

7.1. Soliton trains

It is established for a long time that when a wave is subjected to a modulation instability, it eventually splits up in a wave train depending solitons type [12–15]. To observe this behavior in our bi-inductance line, we introduced at the entrance of the line a wave whose frequency is located in the region of modulation instability of BF and the mode, which presents an amplitude sufficiently high to cause a strong disturbance that will trigger the phenomenon of MI. We take a signal of frequency as $f = 491.5$ kHz and amplitude $V_M = 4$ V. We put two probes at the cell 74 and the cell 86 to observe the evolution of the wave train. Knowing the frequency of the wave and the wave number through the dispersion curve, we determine the phase of the wave speed thanks to the equation (Eq. (1)), we obtain: $f = 491.5$ KHz, $k = 1.21$ rad./cel., by the dispersion curve, and $v_\varphi = 2.55 \times 10^6$ cel/s.

This indicates that the wave crosses a cell in 0.39×10^{-6} s and (86–74) cells or 12 cells closer than 5 ms. This value allows us to identify a particular point of the wave collected at the 74th cell and determine its new position on the waveform of the 86th cell. We present, in **Figure 21**, the waveform of signals collected at the cells 74 and 86. We see in the figure, the train of solitons, which run through the line. We identify a shoulder (cursor C1) which is the waveform corresponding to the signal collected at the 74th cell, which corresponds to two solitons which follow. The cursor positioned on the soliton of greater amplitude. The cursor positioned at 5 ms, (cursor C2) shows the new position of the two solitons. We find that the highest amplitude of soliton exceeded the lowest amplitude of soliton. This observation is in agreement with the results of simulations and observations made on the solitons confirms that the speed of propagation of a soliton is more important than its amplitude [2].

7.2. Propagation of a solitary wave in the line

The image of the optical solitons, which are the natural optoelectronics bits, can be designed as electric solitons that present a sech2 profile in the time domain. We have therefore built a signal whose profile is given by the relationship (Eq. (4)):

$$V(t) = A \operatorname{sech}^2(\alpha t) \quad (4)$$

where A and α are adjustable parameters and t time.

We inject into the bi-inductance line a signal in sech^2 profile, and we follow the evolution of the signal in the line. We observe, in **Figure 22**, the evolution of signal at input cell 72 and input cell 144. We note that the shape of the signal remains intact during its spread in the line. However, we are seeing a weakening of the amplitude that is bound to the dissipative nature of the line. On the other hand, just like Remoissenet [2], we observe an oscillatory tail that accompanies the solitary wave in its spread.

7.3. Shape modification of the signal

As we previously announced in [18], the LTNL can be used to modify the forms of signals. One example is in the case of the generation of radar abrupt front signals to obtain systems that are more accurate. Even our experimental line is not designed and optimized to produce that effect. We have been able to observe some modification in waveforms by nonlinearity.

7.3.1. Signal compression

To illustrate the phenomenon of signal compression, we inject a sinusoidal wave amplitude $V = 1.75 \text{ V}$ for a voltage polarization of the line $V_0 = 1.5 \text{ V}$ and frequency $f = 169.4 \text{ KHz}$, at the entrance of the line. We observe at the 101th cell, the signal compared to the starting signal as a factor of compression order 2 (**Figure 23**).

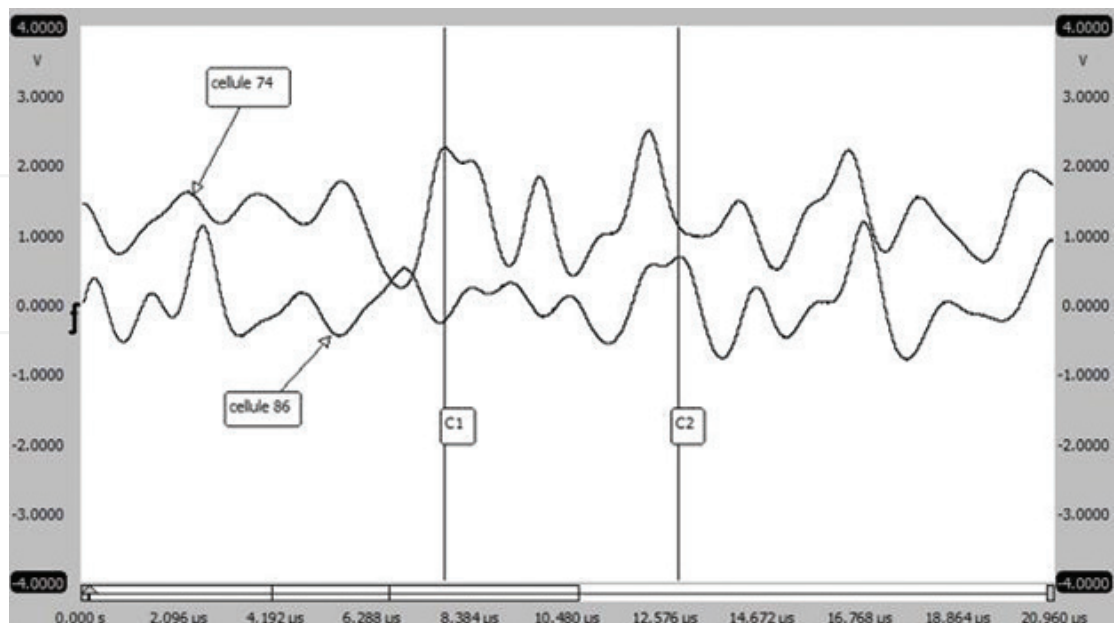


Figure 21. Observation of a train of soliton produced by the fragmentation of a plane wave subject to modulation instability for the BF of 491 kHz frequency and amplitude 4 V. The positions of the C1 and C2 sliders allow seeing the evolution of a pair of soliton in the line at cell 74 and cell 86.

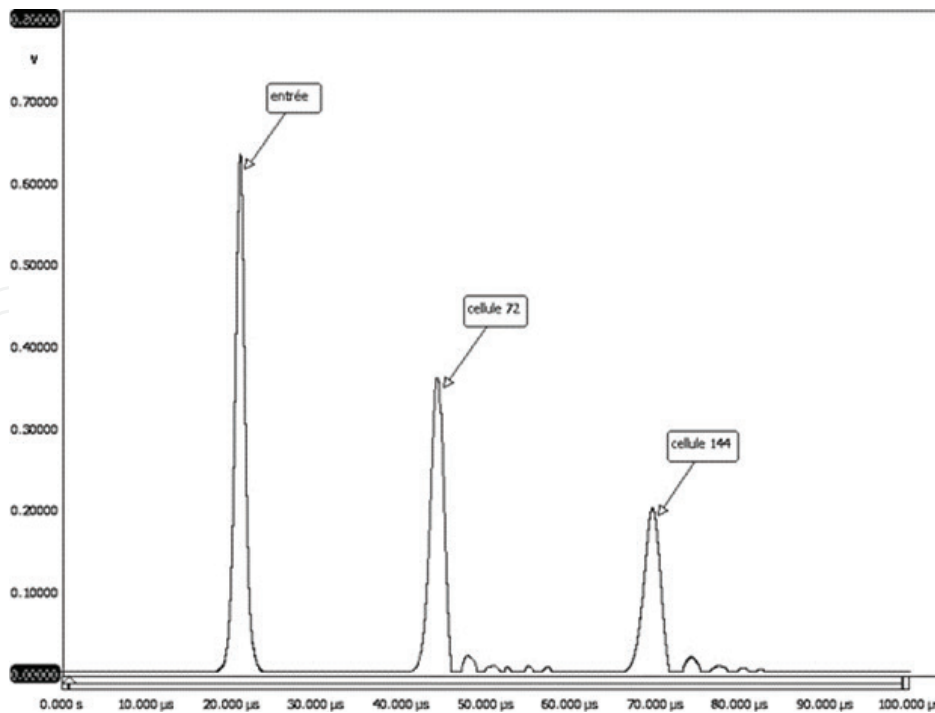


Figure 22. Evolution of a solitary wave sech2 profile in the bi-inductance line. Note the conservation of cohesion of the wave; the decrease amplitude is due to losses by Joule effect and the presence of the oscillatory tail.

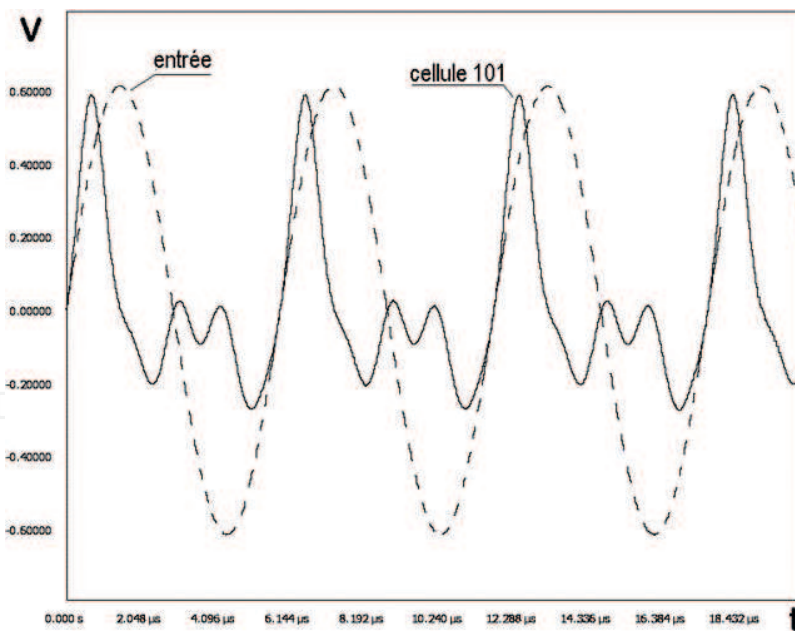


Figure 23. Compression of a signal effect observed in the cell 101 (full lines) for an input signal of sinusoidal form $f = 169.4$ KHz frequency and amplitude $V = 1.75$ V (dashed), polarization of the line voltage is $V_0 = 1.5$ V.

7.3.2. Frequency multiplier

Generally to raise the frequency in electronic systems, it is necessary to use oscillators which present increasingly raised (brought up) frequencies of vibration. Since a few years, the NLTL combined with an amplifier, which amplifies the signals stemming from the noise of the electronics.

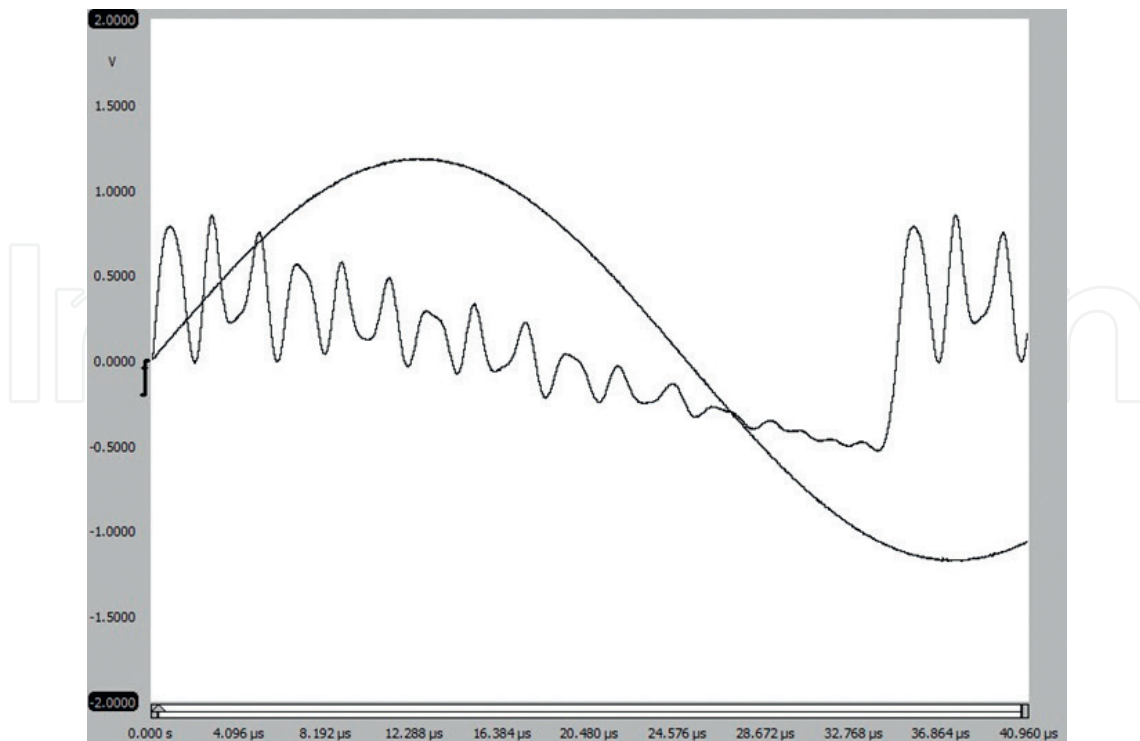


Figure 24. Decomposition of a half period of a sine wave of amplitude $V = 1.5$ V and $f = 20$ KHz frequency, in a solitary wave train observed the cell 175 for a voltage polarization $V_0 = 1.5$ V.

For what concerns us, we show the feasibility of the project by proposing another approach. We had shown in Section 2 that the nonlinearity could produce a shock wave on a sinusoidal signal injected in the NLTL (**Figure 7** in Section 4). If we bring this phenomenon, we show that it is possible to decompose a given plane wave of frequency $f = 20$ KHz at wave train alone. We show (**Figure 24**) that the half-life of the initial sine wave consists of the solitary wave train, which was observed at the 175th cell. Everything happens if the system increases the frequency of the original wave by a new wave train, which has the frequency greater than the starting frequency.

8. Conclusion

We present in this work a selection of experimental results which we reached and which concerns essentially the system of study of our choice, worth knowing, the electrical nonlinear transmission line.

We notice that our experimental device was proved to be a powerful tool of work characterized by its flexibility and its robustness. Qualities essentially owed to our strategic choice who allowed us to make our investigations on sections of lines in the modest size by comparison to other systems constituted by hundreds or even thousands of cells. This arrangement also allowed us to reduce considerably the sources of drift or of artifacts, which increase with the number of components of the line.

From the point of view of the experimental results, we determined, at first, experimentally the dispersion curve of the line by an original method, which consists of determining the phase

velocity of the wave between two consecutive cells. We determine the dispersion curve with a very good precision.

We proof the reality of the transmission of the waves in electrical lines not shelf spaces. We observed the effects of the waste and the dispersion of the waves. On the other hand, even our device was not designed and optimized to produce certain effects on the signals; we observed the modification of the shape of the signals like the compression of signal and the multiplication (increase) of frequency.

Finally, it is recognized today unanimously that the nonlinear physics was born with the remarkable work of Fermi, Pasta, and Ulam, who concerned an abstract system and the study which was made by numeral calculation, the collection what it was advisable today to call the FPU recurrence is a constant current events whatever is the system. We observed the FPU recurrence in the NLTL in BF mode and in HF mode. Hence, we brought a completely original explanation that gets off the beaten track.

The device carried out during this work makes possible to carry out in future work on the investigations on the nonlinear transmission lines and on the dynamics of the solitary waves in various applications as: characterization of the periodical loaded transmission lines, use of the nonlinear reactance of thin layers superconductive, resolution of the Ginzburd-Landau equations for a tangential magnetic field, supraconductivity in the forbidden band in a bimodal nonlinear system; and so on.

Acknowledgements

We thank CEA-MITIC/UFR SAT/UGB for their financial support for the publication of this work.

Author details

Abdou Karim Farota^{1*}, Mouhamadou Mansour Faye², Bouya Diop¹, Diène Ndiaye¹ and Mary Teuw Niane¹

*Address all correspondence to: abdou-karim.farota@ugb.edu.sn

1 UFR SAT, University of Gaston Berger of Saint-Louis, Senegal

2 FST, University Cheikh Anta Diop of Dakar, Senegal

References

- [1] Pelap FB. Dynamique des ondes modulées dans les lignes électriques non linéaires [thesis]. Université Chekh Anta Diop de Dakar (UCAD); 2004
- [2] Remoissenet M. Waves Called Solitons: Concepts and Experiments. New York: Springer-Verlag; 1999. 103p
- [3] Case MG. Nonlinear transmission lines for picosecond pulse, impulse and millimeter-wave harmonic generation [dissertation]. Santa Barbara: University of California; 1993

- [4] Ricketts DS et al. Electrical solitons oscillator. *Transaction on Microwave Theory and Techniques*. 2005;**54**(1):373-382
- [5] Ham D et al. Ordered and chaotic electrical solitons: Communication and perspectives. *IEEE Communications Magazine*. 2006;**44**(12):126-135
- [6] Genie F, Leon J. Supratransmission nonlinéaire dans la bande interdite. In: *Rencontre du Nonlinéaire*. 2002. pp. 119-123
- [7] Adcock TAA, Taylor PH. Focusing of unidirectional wave groups on deep water: An approximate nonlinear Schrödinger equation based-model. *Proceedings of the Royal Society*. 2009;**0224**:3083-3102. DOI: 10.1098/rspa 2009
- [8] Benjamin TB. Instability of periodic wave trains in nonlinear dispersive systems. *Proceedings of the Royal Society of London, Series A*. 1967;**299**:59-75
- [9] Scott Russel J. Report on waves. In: *Report on the Fourteenth Meeting of British Association for Advancement of Science*; 1844. 57 plates. pp. 311-390
- [10] Darcy H, Bazin H. *Recherches Expérimentales sur L'écoulement de l'eau dans les Canaux Ouverts*. *Recherches Hydrauliques Entreprises*. Paris: Imprimerie Impériale, M DCCCLXV, Dunod; 1865
- [11] Boussineq J. *Esaie sur la théorie des eaux courantes* [thesis]. *Mémoires présentés par divers savants de l'Academie des Sciences: Institut National de France*; 1877. pp. 1-680
- [12] Marquié P, Bilbault JM, Remoissenet M. Nonlinear Schrödinger models and modulational instability in real electrical lattices. In: *The Nonlinear Schrödinger Equation Achievements, Developments, Perspectives (NLS 94)*. Chernogolovka, Russia; 1994
- [13] Gaetan VS. *Instabilité, solitons et solhiatons, une approche expérimentale de la dynamique non linéaire en fibres optiques* [thesis]. Université Libre de Bruxelles; 2003
- [14] Klinger J, Martin H, Chen Z. Experiments on induced modulational instability of an incoherent optical beam. *Optics Letters*. 2001;**26**(5):271-273
- [15] Alfano RR. *The Supercontinuum Laser Source: The Ultimate White Light*. New York: Springer; 2016. 434p
- [16] Lange CG, Newell AC. A stability criterion for envelope equations. *SIAM Journal on Applied Mathematics*. 1974;**27**:441-456
- [17] Fermi E, Pasta J, Ulam HC, Tsingou M. (Pré-rapport du 7 novembre 1955). In: *Collected Papers (Note e Memorie)*. 1955; Vol. II - United States 1939-1954, Segrè E, editor. The University of Chicago. pp. 977-988
- [18] Farota AK. *Etude et mise en oeuvre d'une ligne de transmission électrique non linéaire* [thesis]. Université Gaston Berger de Saint-Louis (UGB); 2015
- [19] Farota AK, Faye MM. Experimental study of the Fermi-Pasta-Ulam recurrence in a bimodal electrical transmission line. *Physicq Scriptq*. 2013;**88**(5):055802
- [20] Toda M. Studies of a non-linear lattice. *Physics Reports*. 1975;**18C**:1-124

